



Hadronic γ -ray emission from extragalactic mini radio lobes

M. Kino^{1*} and K. Asano²

¹ National Astronomical Observatory of Japan, Tokyo 181-8588, Japan

² Interactive Research Center for Science, Tokyo Institute of Technology, Tokyo 152-88550, Japan

Abstract.

Hadronic emission from parsec size radio lobes in active galactic nuclei (AGN) is discussed. The lobes are composed of shocked jet plasma and expected to be filled with high energy particles. By using the Monte Carlo simulation, we calculate the photon spectra from the lobes including photo-meson interaction processes. When the synchrotron emission from primary electrons is bright, synchrotron-self-Compton component is dominant in γ -ray bands. The hadronic emission from the lobes can be dominated in γ -ray bands when the primary emission is not very bright. Proton synchrotron component arises at sub MeV band. The synchrotron emission radiated from secondary e^\pm pairs produced via photo-meson cascade emerges in \sim GeV-TeV energy ranges. These high energy emission signatures provide a test for proton accelerations in young AGN jets.

1. Introduction

The progress of VLBI (Very Long Baseline Interferometry) observations reveal the existence of compact radio-loud active galactic nuclei (AGN) with its linear size $LS < 1$ kpc (e.g., Readhead et al. 1996; O’Dea & Baum 1997). These compact radio sources are currently understood as young progenitor of large radio galaxies (e.g., Fanti 2009 for review). Furthermore, recent investigations discover smaller radio lobes with $LS \sim \mathcal{O}(10)$ pc (e.g., Snellen et al. 2004; Orienti et al. 2008). It is well known that recurrent radio sources also possess mini lobes inside them (e.g., Walker et al. 2000). High energy emissions from these compact radio sources have been recently explored by some authors (e.g., Stawarz et al. 2008; Kino et al. 2009). However, the previous works focus on the leptonic emissions and little is known about a hadronic emission in them.

Since mini radio lobes with $LS \sim 10$ pc are closely located near the AGN core, the lobes are expected to be in dense external radiation fields (Fig. 1). Furthermore, together with electrons, the shocks accelerate protons as well. Therefore high energy protons are naturally expected to be filled with the radio lobes although its total amount is still unknown. Therefore $p\gamma$ interaction is inevitable for the mini lobes. Here, we examine $p\gamma$ interactions between high energy protons and surrounding target photons. As for external photons, we focus on UV photons from the standard accretion disks.

2. Model

Following the standard picture of radio lobe formation in AGNs (e.g., Begelman et al. 1984), here we briefly review the standard picture of radio lobes. When a jet interacts with surrounding ambient matter, most of its kinetic energy is dissipated via strong shocks. The termination point

at the tip of the jet is called as hot spots. The hot spot is identified as the reverse shocked region of the decelerated jet. The shocked jet plasma leak from the hot spot and they form radio lobes. Therefore we can say that the radio lobes are the remnant of the decelerated jets which contain relativistic particles. In this work, we examine the case when the lobe contains relativistic protons.

2.1. Proton acceleration and coolings

Hot spots in powerful radio galaxies are one of the promising sights for proton acceleration (e.g., Rachen and Biermann 1993). Here we show that hot spots in mini lobes are also plausible sights for proton acceleration. Hereafter the maximum energy of shock accelerated protons is denoted as $E_{p,\max} = \gamma_p m_p c^2$. The proton acceleration time scale at the hot spots $t_{p,\text{acc,hs}} = \xi_p E_p / (e B_{\text{hs}} c)$ is estimated as

$$t_{p,\text{acc,hs}} \approx 3.5 \left(\frac{\xi_p}{100} \right) \left(\frac{E_p}{10^{18} \text{ eV}} \right) \left(\frac{B_{\text{hs}}}{10^{-1} \text{ G}} \right)^{-1} \text{ yr}, \quad (1)$$

where B_{hs} , and ξ_p are the magnetic field strength, and the ratio of the acceleration timescale and Larmor timescale for protons at the hot spot, respectively. Although there is no direct estimate for B_{hs} , the magnetic field strength in mini lobes (B) have been recently estimated as $B \sim 10 - 100$ mG by VLBI observations (Orienti et al. 2008). Since the magnetic field strength at the hot spot B_{hs} should be comparable or larger than B . Here we set $B_{\text{hs}} \sim 100$ mG. The value of ξ_p is a free parameter. For blazars, it is constrained as $\xi_p > 10$ (Aharonian et al. 2002). There is little constraint on ξ_p for hot spots in mini lobes and we examine the case of $\xi_p = 100$ in this work. The timescale of proton synchrotron is $t_{p,\text{syn,hs}} = (6\pi m_p^4 c^3) / (\sigma_T m_e^2 E B^2) \approx 1 \times 10^4 (E_p / 10^{18} \text{ eV})^{-1} (B_{\text{hs}} / 0.1 \text{ G})^{-2}$. The high energy protons escape from the hot spots via sideways expansions and they are injected into the mini lobes. When the

* motoki.kino@nao.ac.jp

escape velocity from the hot spot is $\sim 0.3 c$, the escape timescale is accordingly $t_{\text{esc,hs}} \sim 3 (R_{\text{hs}}/10^{18} \text{ cm})$ years. Therefore, the typical $E_{p,\text{max}}$ is obtained by the relation $t_{p,\text{acc,hs}} \approx t_{\text{esc,hs}}$ and it is

$$E_{p,\text{max}} \approx 1 \times 10^{18} \left(\frac{\xi_p}{100} \right)^{-1} \left(\frac{R_{\text{hs}}}{10^{18} \text{ cm}} \right) \left(\frac{B_{\text{hs}}}{10^{-1} \text{ G}} \right) \text{ eV} \quad (2)$$

The Larmor radius of high energy protons with $E_p \sim 10^{18} \text{ eV}$ is sufficiently smaller than R_{hs} . Hence, the conditions of proton acceleration are satisfied.

Next, high energy protons escape from the hot spot via sideways expansions and they injected in the mini lobes. Then, they undergo various coolings in the lobes, i.e., adiabatic loss, $p\gamma$ interaction, and proton synchrotron cooling. Below, we calculate these processes with the Monte Carlo simulation.

3. Monte Carlo simulation

To calculate broadband photon spectra, the Monte Carlo simulation has been performed in this work. The numerical code has been developed by Asano et al. (2008, 2009) and references therein. Therefore we do not repeat it here. Details are shown in Kino and Asano (2010). Distributions of particles and photons are assumed to be isotropic. We include the following physical processes: (1) photopion production from protons and neutrons ($p + \gamma \rightarrow p/n + \pi^0/\pi^\pm$), (2) pion decay ($\pi^0 \rightarrow 2\gamma$), ($\pi^\pm \rightarrow \mu^\pm + \nu$) and muon decay ($\mu^\pm \rightarrow e^\pm + \nu$), (3) photon-photon pair production ($\gamma + \gamma \rightarrow e^+ + e^-$), (4) Bethe-Heitler pair production ($p + \gamma \rightarrow p + e^+ + e^-$), (5) synchrotron and inverse Compton processes of electrons/positrons, protons, pions, muons with Klein-Nishina cross section, (6) synchrotron self-absorption for electrons/positrons, and (7) adiabatic expansion loss.

4. Results

Fig. 2 shows the photon spectra for the case of $L_e = 1 \times 10^{45} \text{ erg s}^{-1}$, $1 \times 10^{44} \text{ erg s}^{-1}$, $1 \times 10^{43} \text{ erg s}^{-1}$, $1 \times 10^{42} \text{ erg s}^{-1}$, and $1 \times 10^{41} \text{ erg s}^{-1}$ where L_e is the injection power of non-thermal electrons. For electron Gyrofactor, we set $\xi_e = \xi_p = 1 \times 10^2$. The injection index is assumed as $s = 2$ both for electrons and protons. Based on VLBI observations, we set the following parameters as $R = 2 \text{ pc}$, $R_{\text{hs}} = 0.3 \text{ pc}$, $B = 0.1 \text{ G}$, $v_{\text{exp}} = 0.1 c$, $LS = 10 \text{ pc}$, and $\gamma_{p,\text{min}} = \gamma_{e,\text{min}} = 10$. As for the luminosity and temperature of the standard accretion disk, we assume $L_{\text{disk}} = 3 \times 10^{45} \text{ erg s}^{-1}$, and $kT_{\text{disk}} = 10 \text{ eV}$ (e.g., Ostorero et al. 2009). We impose a injection power of high energy protons L_p being smaller than total kinetic powers of powerful radio galaxies $\sim 10^{47-48} \text{ erg s}^{-1}$ (e.g., Ito et al. 2008). We assume $L_p = 5 \times 10^{46} \text{ erg s}^{-1}$ in this work.

Thin solid lines in Fig. 2 shows the photon spectra without proton injection (i.e., $L_p = 0$). The synchrotron spectra from the primary electrons are well studied by VLBI observations. The turnover frequency is mainly caused by synchrotron self absorption (SSA) (e.g., Snellen

et al. 2000). According to the synchrotron luminosity of the mini lobe L_{syn} , the observed turnover frequencies of mini lobes show $\nu_{\text{SSA}} \sim 0.1 - 10 \text{ GHz}$. At the same time, primary electrons suffer from fast synchrotron cooling. Therefore a break frequency due to the synchrotron cooling typically appears comparable to or below ν_{SSA} . This implies that $L_e \approx L_{\text{syn}}$.

Thick solid lines in Fig. 2 represent the photon spectra with proton injection. It is found that the amount of primary electrons controls whether hadronic emission is visible or not. For the lobe with $L_e = 1 \times 10^{45} \text{ erg s}^{-1}$, the leptonic emissions overwhelm the hadronic emissions at all energy domains. As a result, the spectrum with proton injection is almost the same as the one without protons injection. Therefore, the bright lobe is not suitable for testing the existence of high energy protons. As L_e decreases to $L_e \leq 1 \times 10^{44} \text{ erg s}^{-1}$, thick and thin lines become separable at γ -ray energy range because synchrotron emission from secondary electrons is added in the thick lines. For the lobes with $L_e < 1 \times 10^{43} \text{ erg s}^{-1}$, the proton synchrotron bump appears in sub-MeV range with the peak at

$$\nu_{p,\text{syn}} \approx 0.7 \left(\frac{E_p}{10^{18} \text{ eV}} \right)^2 \left(\frac{B}{10^{-1} \text{ G}} \right) \text{ MeV}. \quad (3)$$

In TeV energy range, it is shown that TeV- γ photons are significantly attenuated due to soft photons in the lobes.

5. Summary

Hadronic emission at extragalactic mini radio lobes is discussed in this work. We calculate the broadband photon spectra taking $p\gamma$ interaction and proton synchrotron cooling into account. The powers of standard accretion disk and injected protons are $L_{\text{disk}} = 3 \times 10^{45} \text{ erg s}^{-1}$, $L_p = 5 \times 10^{46} \text{ erg s}^{-1}$, respectively.

For bright lobes with $L_e \sim L_{\text{syn}} \sim 10^{45} \text{ erg s}^{-1}$, the predicted VHE emission is detectable with *Fermi*/LAT, and HESS. Since it is overwhelmed by the leptonic components in this case, it is hard to figure out whether the γ -ray emission is hadronic- or leptonic-origin. For the lobe with $L_e \sim 10^{44} \text{ erg s}^{-1}$, secondary e^\pm pairs radiate TeV γ synchrotron emission and it is detectable by the current TeV γ telescopes.

For less luminous radio lobes $L_e \sim L_{\text{syn}} < 10^{44} \text{ erg s}^{-1}$, the proton synchrotron bump appears at sub MeV energy band. The synchrotron bump from secondary e^\pm pairs created by μ -decay appears at GeV/TeV ranges. If the double bumps due to these hadronic processes are detected, it would be a support for the hadronic model since leptonic model does not easily account for such double bumps.

6. Future prospects

We add to comment on the recent radio observation of mini lobe 3C 84 which is associated with NGC 1275 ($z = 0.0176$). It shows the outburst around 2005 and the

new component C3 emerges with the size smaller than 1 pc (Nagai et al. 2010). *Fermi*/LAT also detect GeV γ -ray emission in the same period (Abdo et al. 2009). Fig. 3 displays the actual multi-epoch images of 3C 84 obtained by VERA observations at 22 GHz (Nagai et al. 2010). While the flux of C3 component measured by VERA increases, GeV γ -ray flux over the period August 2008 - August 2009 seems to remain constant (Kataoka et al. 2010). The difference of the measured flux variations between VLBI and *Fermi*/LAT could indicate a breakdown of the one-zone synchrotron-self Compton model proposed in Abdo et al. (2009). Hadronic emissions could partly contribute in γ -ray energy bands, although we did not deal with the specific case of 3C 84 in this work. In order to nail down the real γ -ray emitter, continuous observations by VLBI are quite important.

In the near future, the project of VLBI Space Observatory Programme-2 (VSOP-2) with the high angular resolution (Tsuboi et al. 2009) will play a unique role for mini lobe observations. Observations will be made with the 9-m antenna in orbit together with ground radio telescopes, and will achieve the angular resolutions of 40, 80, and 210 microarcsec at 43, 22, and 8 GHz, respectively. Especially, observations at 8 GHz will unveil fine structures of unresolved mini lobes. Furthermore, the era of VSOP-2 will overlap the duration in which the next generation TeV γ -ray telescope *CTA* would be in operation (<http://www.cta-observatory.org/>). *CTA* will have a factor of 5-10 improvement in sensitivity in the current energy domain of about 100 GeV to some 10 TeV and an extension of the accessible energy range well below 100 GeV and to above 100 TeV. A future collaboration between VSOP-2 and *CTA* will be one of the best ways to explore the origin of γ -ray emission from mini radio lobes.

Acknowledgements. We are indebted to H. Nagai for providing us the image in Fig. 3.

References

- Abdo, A. A., et al., 2009, *ApJ*, 699, 31
 Aharonian, F. A., Belyanin, A. A., Derishev, E. V., Kocharovskiy, V. V., & Kocharovskiy, V. V., 2002, *PhRvD*, 66, 023005
 Asada, K., Kamenou, S., Shen, Z.-Q., Horiuchi, S., Gabuzda, D. C., & Inoue, M., 2006, *PASJ*, 58, 261
 Asano, K., & Mészáros, P., 2008, *ApJ*, 677, L31
 Asano, K., Guiriec, S., & Mészáros, P., 2009, *ApJ*, 705, L191
 Begelman, M. C., Blandford, R. D., & Rees, M. J., 1984, *RvMP*, 56, 255
 Fanti, C., *AN*, 330, 120
 Giroletti, M., & Polatidis, A., 2009, *AN*, 330, 193
 Ito, H., Kino, M., Kawakatu, N., Isobe, N., & Yamada, S., 2008, *ApJ*, 685, 828
 Kataoka, J., et al., 2010, *ApJ*, 715, 554
 Kino, M., Ito, H., Kawakatu, N., & Nagai, H., 2009, *MNRAS*, 395, L43
 Kino, M., & Asano, K., 2010, in preparation
 Nagai, H., et al., 2010, *PASJ*, 62, L11
 O’Dea C. P., Baum S. A., 1997, *AJ*, 113, 148

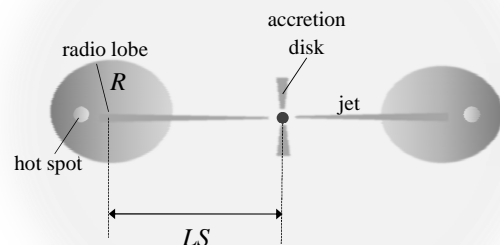


Fig. 1. A cartoon of mini radio lobes immersed in radiation field due to the accretion disk. In this work, we examine the case of $R = 2$ pc, $LS = 10$ pc and $L_{\text{disk}} = 3 \times 10^{45}$ erg s $^{-1}$.

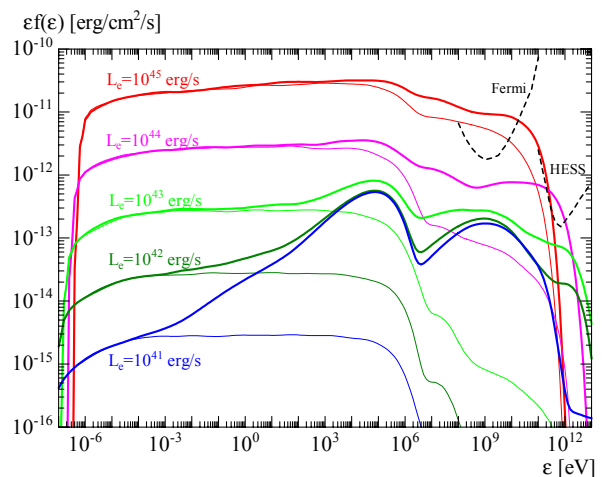


Fig. 2. Predicted broadband spectra from the mini radio lobe for $L_p = 5 \times 10^{46}$ erg s $^{-1}$ and $L_{\text{uv}} = 3 \times 10^{45}$ erg s $^{-1}$. Black, green, yellow, red, and blue lines are the case for $L_e = 1 \times 10^{45}$ erg s $^{-1}$, 1×10^{44} erg s $^{-1}$, 1×10^{43} erg s $^{-1}$, 1×10^{42} erg s $^{-1}$, and 1×10^{41} erg s $^{-1}$, respectively. The lobes are located at the distance $D = 100$ Mpc. The proton synchrotron bump is predicted at \sim sub MeV for smaller L_e .

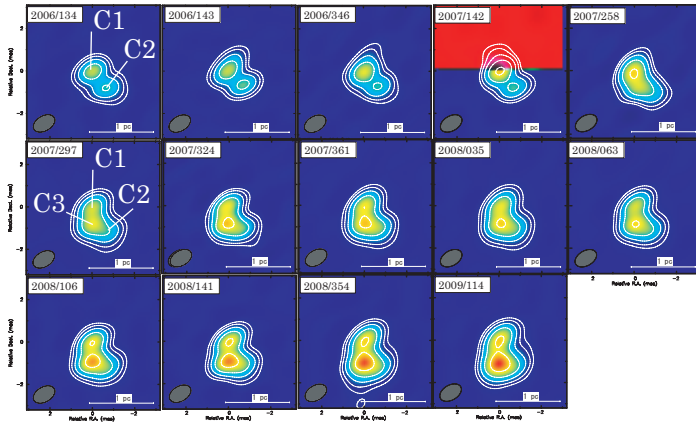


Fig. 3. Multi-epoch VERA images of 3C 84 at 22 GHz. The C1 component is assumed to be the core. The C3 component is the new born one and it proceeds to the south. The size is still less than 1 pc.

- Orienti, M., & Dallacasa, D., 2008, *A&A*, 487, 885
 Ostorero, L., et al., 2009, arXiv, arXiv:0910.3611
 Rachen, J. P., & Biermann, P. L., 1993, *A&A*, 272, 161
 Readhead, A. C. S., Taylor, G. B., Pearson, & T. J., Wilkinson, P. N., 1996a, *ApJ*, 460, 612
 Snellen, I.A.G., Schilizzi, R.T., & Miley, G.K. et al. 2000, *MNRAS*, 319, 445
 Snellen, I. A. G., Mack, K.-H., Schilizzi, R. T., & Tschager, W., 2004, *MNRAS*, 348, 227
 Stawarz, L., Ostorero, L., Begelman, M. C., Moderski, R., Kataoka, J., & Wagner, S., 2008, *ApJ*, 680, 911
 Tsuboi M., et al., 2009, ASP Conf. Ser. 'Approaching Micro-Arcsecond Resolution with VSOP-2: Astrophysics and Technology', eds. Y. Hagiwara, E. Fomalont, M. Tsuboi, and Y. Murata, 402, 30
 Walker, R. C., Dhawan, V., Romney, J. D., Kellermann, K. I., & Vermeulen, R. C., 2000, *ApJ*, 530, 233